Synthetic Metals 173 (2013) 22–25

Contents lists available at SciVerse ScienceDirect

Synthetic Metals

journal homepage: www.elsevier.com/locate/synmet

High spin polarization at the Fe/C_{60} interface in the Fe-doped C_{60} film

Seiji Sakai[a,*], Yoshihiro Matsumoto[a], Manabu Ohtomo[a], Shiro Entani[a], Pavel V. Avramov[a], Pavel B. Sorokin[a,b], Hiroshi Naramoto[a]

[a] Advanced Science Research Center, Japan Atomic Energy Agency, 2-4 Shirakata-Shirane, Tokai, Naka 319-1195, Japan
[b] Technological Institute of Superhard and Novel Carbon Materials, 7 a Centralnaya Street, Troitsk, Moscow Region 142190, Russian Federation

ARTICLE INFO

Article history:
Received 1 October 2012
Received in revised form 24 October 2012
Accepted 29 October 2012
Available online 20 December 2012

Keywords:
Fullerene
Magnetic metal
TMR effect
Spin polarization
Spinterfaces

ABSTRACT

A process of tunneling conduction and the spin-dependent resistivity change (so-called tunneling magnetoresistance effect) in the Fe-doped C_{60} film with a granular structure is investigated for the current-into-plane device. Cooperative tunneling (cotunneling) through several Fe nanoparticles is suggested to be operative at temperatures lower than 20 K. By considering the effect of cotunneling on the magnetoresistance ratio, it is successfully shown that the spin polarization of tunneling electrons generated at the Fe/C_{60} interface is much higher than that in Fe crystal at low temperature in a similar fashion to that at the Co/C_{60} interface in the Co-doped C_{60} films. A strong temperature dependence of spin polarization is observed, suggesting a possible influence by the thermally induced disorders ascribed to the Fe atoms bonded with C_{60} in the C_{60}—Fe compound.

1. Introduction

Molecular materials (MMs) including π-conjugated organic molecules and nanocarbons are expected to offer a great potential for the development of nano-spintronic devices. In order to explore the spintronic applications of MMs, considerable attention has been focused on the efficient spin-injection from ferromagnetic metal (FM) contacts that is the most fundamental aspect of spintronics. Although the MM/FM interface would have a predominant role in the spin-injection efficiency and is attracting attention as "spinterface" [1], the details of spin polarization at the MM/FM interface are scarcely known due to the difficulty in fabricating magnetoresistive spin-valve devices with well-defined structures, and more fundamentally due to insufficient information on the material states and properties of the interfaces [2–4]. Recent spectroscopic and theoretical studies [5–9] have pointed out that the interface interactions cause significant changes in electronic and magnetic structures of the MM/FM interfaces, which possibly depend on the species of FM as well as MM. Previously, we have successfully demonstrated that the magnitude of the interface spin polarization (P_{int}) can be remarkably high compared to that in FM based on the analysis of the spin-dependent tunneling in the cobalt (Co)-doped C_{60} films with a granular structure of a C_{60}-based insulating matrix and well-dispersed Co nanoparticles [10–12]. In the present study, we conducted a comparative study on the spin-dependent transport property of the iron (Fe)-doped C_{60} film for the sake of gaining additional insights into the spin polarization at the interface between C_{60} and FM by changing the FM species from Co to Fe.

2. Experimental

A Fe-doped C_{60} film was fabricated by using the co-deposition method in UHV. C_{60} (99.99% purity, sublimed grade) and Fe (99.99% purity) were deposited on a mirror-polished MgO(0 0 1) substrate from a Knudsen cell and an electron-beam (EB) evaporator, respectively, in the vacuum of 10^{-7} Pa. A two-terminal device with the current-into-plane (CIP) geometry was prepared by depositing a Fe-doped C_{60} film with a film composition of $C_{60}Fe_7$ and with thickness of 100 nm on a pair of 50 nm thick platinum (Pt) electrodes with a 40 μm separation. The film composition was determined from the thickness of the areas of pure C_{60} and pure Fe which were simultaneously deposited by using shadow masks. The surface of the CIP device was coated with a 100 nm thick aluminum oxide (AlO) layer for preventing oxidation. The chemical state and magnetic property of the $C_{60}Fe_7$ film were checked utilizing a micro-Raman spectrometer (Nano-Finder, Tokyo Instruments) and SQUID magnetometer (MPMS, Quantum Design) for the AlO coated samples, respectively. Raman measurements were performed using the 488 nm line of an argon-ion laser in a backscattering geometry. Spin-dependent transport property of the CIP device under an in-plane magnetic field (H) was investigated in the temperature (T) range of 1.9–100 K by using the SQUID

* Corresponding author. Tel.: +81 29 282 6582; fax: +81 29 282 5927.
E-mail address: sakai.seiji@jaea.go.jp (S. Sakai).

0379-6779/$ – see front matter © 2012 Elsevier B.V. All rights reserved.
http://dx.doi.org/10.1016/j.synthmet.2012.10.027

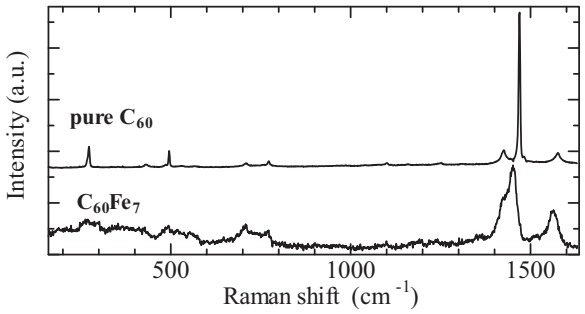

Fig. 1. Raman spectrum of the $C_{60}Fe_7$ film and that of a pure C_{60} film for comparison.

magnetometer. Throughout this study, the pessimistic definition of the MR ratio is employed as $MR(H) = (R_{max} - R(H))/R_{max}$, where $R(H)$ and R_{max} are the electrical resistances at the arbitrary magnetic field and also at the maximum, respectively.

3. Results and discussion

A Raman spectrum of the $C_{60}Fe_7$ film is represented in Fig. 1 together with that of a pure C_{60} film for comparison. Although, a C_{60} molecule with the icosahedral (I_h) symmetry has only 10 Raman active modes (8 H_g modes and 2 A_g modes), one can recognize much more peaks in the spectrum of the $C_{60}Fe_7$ film. Obvious shifts of the Raman peak positions compared to those in pure C_{60} are observed for the $A_g(2)$ and $H_g(8)$ modes; the $A_g(2)$ peak (1452 cm^{-1}) and the $H_g(8)$ peak (1564 cm^{-1}) for $C_{60}Fe_7$ are down-shifted by 18 cm^{-1} and 13 cm^{-1} compared to pure C_{60}. The appearance of the numerous peaks and the down-shifts of the $A_g(2)$ and $H_g(8)$ peaks are attributed to the symmetry lowering of C_{60} by the covalent bond formation associated with the π-d hybridization and a charge transfer between the Fe atom to C_{60}, respectively, as analogous to the C_{60}—Co compound [13]. It is noteworthy that peak components characteristic to the oxidized compound [13] are not recognized in the $H_g(8)$ and $A_g(2)$ regions. The magnetization measurement suggests the existence of Fe nanoparticles with a low blocking temperature (7 K) and a high saturation magnetization (>1.0×10^4 emu/mol) which appears to be higher than that of bulk bcc-Fe. Such magnetization behaviors are possibly attributed to the Fe nanoparticles with sizes less than a few nm [14]. Therefore, it is reasonable to interpret that the $C_{60}Fe_7$ film has a granular structure composed of the C_{60}—Fe compound matrix and small Fe nanoparticles.

Fig. 2 displays the current–voltage (I–V) characteristics of the $C_{60}Fe_7$ film measured at different temperatures. A transition from a linear I–V relationship to a power-law one is observed when the voltage increases higher than about $V = 10$ V. As can be seen from

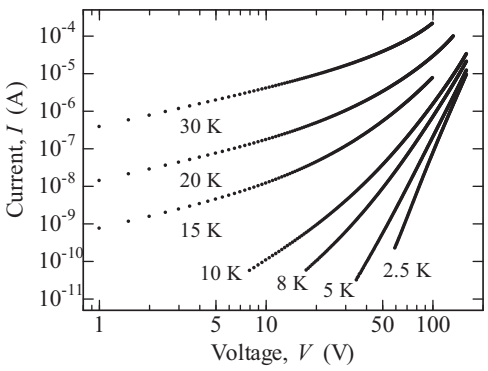

Fig. 2. Current–voltage characteristics of the 100-nm-thick $C_{60}Fe_7$ film measured under the CIP geometry at different temperatures.

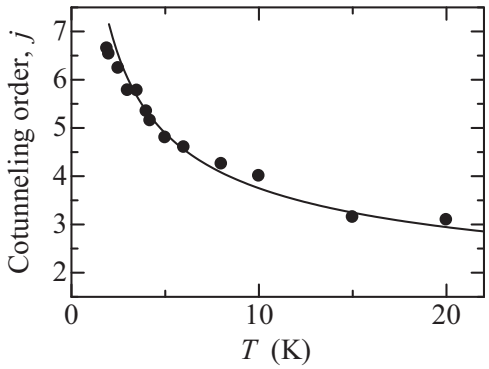

Fig. 3. Cotunneling order j as a function of temperature. The solid line represents the fit with the theoretically proposed dependence for granular systems (see text for details).

this figure, the resistivity (ρ) decreases with increasing temperature. A more detailed analysis shows that ρ under a small voltage follows the characteristic relation ($\rho \propto T^{-1/2}$) for tunneling conduction in insulating granular systems in a broad temperature range (not shown). The observed linear and power-law I–V relationships depending on voltage are consistent not only with those for the Co-doped C_{60} films [11,12] but also with those for the granular films of a dodecanethiol matrix and Au nanoparticles with a regular arrangement [15]. In Ref. [15], Trans et al. have demonstrated that these characteristics are due to the occurrence of cooperative tunneling (so-called cotunneling) through several nanoparticles. They have also shown that the order of cotunneling j that is equivalent to the number of metal nanoparticles taking part in an cotunneling event can be derived from the value of exponent α in the power-law I–V relationship ($I \propto V^{\alpha}$): $j = (\alpha + 1)/2$.

In Fig. 3, the cotunneling order j calculated from the above results for the $C_{60}Fe_7$ film is plotted as a function of the temperature. The values of j are in the range of 3–7 at 1.9–20 K. The j–T dependence seems to be in good agreement with the equation $j = \kappa T^{-0.5} + 1$ (κ is a constant) that is proposed based on an analytical model of cotunneling in granular systems [16]. The best-fit line is drawn by the solid line in the figure. The above results show that cotunneling can be a predominant transport process in the granular films whether the films are magnetic or non-magnetic. It can be claimed that the effect of cotunneling must be considered on the analysis of granular TMR at low temperatures.

Fig. 4 displays the MR–V characteristics at $H = 70$ kOe at the similar temperatures. The results show an exponential MR decrease

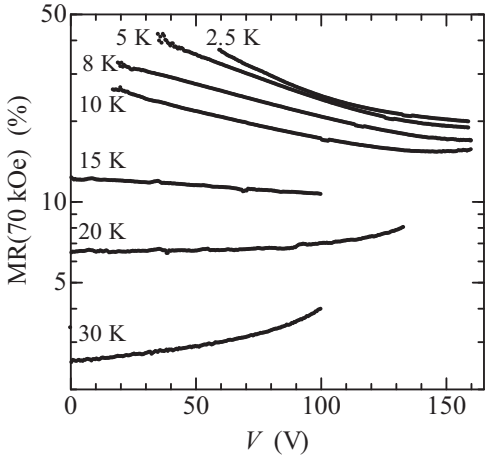

Fig. 4. MR–V characteristics measured at different temperatures.

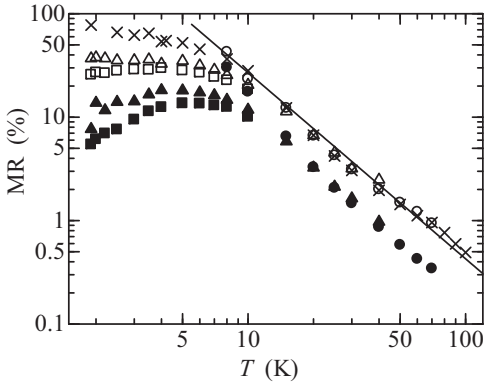

Fig. 5. Plot of the MR ratios at $H = 10$ kOe (solid symbols) and 70 kOe (open symbols) measured under $V = 20$ V (circles), 60 V (triangles) and 80 V (squares) and the zero-bias MR ratio at $H = 70$ kOe (crosses). The measurements were not made in the range of $T < 8$ K at $V = 20$ V and in the range of $T > 10$ K at $V = 80$ V because of the high resistance and the temperature-rise of the device under these conditions.

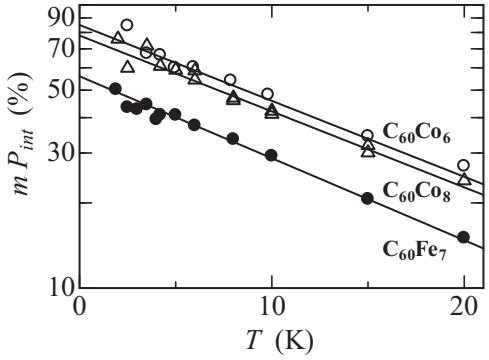

Fig. 6. Interface spin polarization (P_{int}) multiplied by the relative magnetization ($m \leq 1$) of the Fe nanoparticles involved in the transport plotted as a function of temperature. The solid circles, open circles and open triangles represent the data for $C_{60}Fe_7$ (present sample), $C_{60}Co_6$ and $C_{60}Co_8$ (Refs. [11,12]), respectively. The solid lines represent the best-fits to Eq. (2) for the respective samples.

with increasing voltage at lower temperatures than $T = 20$ K. This exponential relationship holds over a wider voltage range depending on the temperature (e.g., $V < 110$ V at $T = 10$ K and $V < 80$ V at $T = 20$ K). Out of the voltage range, MR shows an increase deviating from this relationship ($T < 20$ K) and a monotonic increase with V ($T > 20$ K) and shows a monotonic increase with V at $T \geq 20$ K. Both of the observed I–V and MR–V characteristics are analogous to those reported for the Co-doped C_{60} films in the Coulomb blockade regime.

Fig. 5 shows the temperature dependence of MR at different magnetic fields (10 and 70 kOe) and voltages. The crosses represent MR (70 kOe) at zero voltage given by extrapolating the exponential MR–V relationship into the lower limit. The solid/open circles, triangles and squares represent MR (70 kOe) and MR (10 kOe) measured at $V = 20$, 60 and 80 V, respectively. At higher temperature than $T = 20$ K, the relative magnitude of MR (70 kOe) to MR (10 kOe) is almost constant not depending on temperature and voltage, which means that the shape of the MR curve remains nearly constant, and the MR magnitude is well represented by the relationship: $MR \propto T^{-n}$ ($n = 1.8$). The T^{-n} dependence with n close to 2 is reasonably attributed to the decrease of the spin polarization ($MR \sim P_{int}^2$ in case of $P \ll 1$ and $j \cong 1$) by the paramagnetic localized d-electron spins which would exist in the C_{60}—Fe compound. Meanwhile, the deviation from this relationship becomes obvious when the temperature becomes lower than $T = 20$ K. In this temperature range, the relative magnitude of MR (70 kOe) to MR (10 kOe) shows an increase with decreasing temperature. This is due to the weaker saturation of the MR curve under high magnetic field at lower temperature (not shown). MR (70 kOe) under zero bias and also at various voltages show a saturation tendency at low temperatures. A decrease of MR (10 kOe) with decreasing temperature and which becomes more prominent at higher voltage is seen in the temperature range of $T < 5$ K. Voltage-dependent change in the average size of the Fe nanoparticles taking part in cotunneling may give rise to this phenomena, because in general (co-)tunneling probability in granular films is limited by the Coulomb blockade with particle size-dependent charging energy and hence the smaller Fe nanoparticles with higher electron charging energy and with lower magnetic susceptibility is expected to be involved in the transport under higher voltage.

The cotunneling order j enables us to evaluate the magnitude of the interface spin polarization (P_{int}). According to Takahashi's theory, the zero-bias MR ratio (MR_0) can be expressed as,

$$MR_0 = 1 - (1 + m^2 P_{int}^2)^{-j} \quad (1)$$

where $m = M/M_S$ (M: magnetization, M_S: saturation magnetization). MR_0 is given by extrapolating the exponential MR–V relationship to zero voltage ($T < 15$ K) and approximately as the measured value at $V = 1$ V ($T > 15$ K) considering the weak voltage dependence at near-zero voltage. The magnitude of m for the Fe nanoparticles participated in tunneling conduction would be close to but less than unity even at the highest magnetic field judging from the incomplete saturation of the MR curve (not shown). Therefore, one can obtain the magnitude of the interface spin polarization multiplied by m (≤ 1). Fig. 6 shows mP_{int} as a function of temperature together with the reported values for the Co-doped C_{60} films with metal contents ($C_{60}Co_6$ and $C_{60}Co_8$) nearly identical to the present film ($C_{60}Fe_7$). Two striking features can be seen from this plot. (1) The interface spin polarization is changeable depending on the metal species. (2) The mP_{int}–T relationships are represented employing the following equation with the characteristic temperature $T_C \cong 15$–16 K in common.

$$mP_{int}(T) = mP_{int}(0)\exp\left(\frac{-T}{T_C}\right) \quad (2)$$

The mP_{int} values at zero temperature are 56%, 85% and 78% for $C_{60}Fe_7$, $C_{60}Co_6$ and $C_{60}Co_8$, respectively. These values are remarkably higher compared to the spin polarization in Fe and Co crystals (45% and 42%, respectively) [17] though $P_{int}(0)$ for $C_{60}Fe_7$ appears to be smaller compared to the Co-doped C_{60} films. A more systematic study is required to clarify the effect of metal species. However, as a summary of a series of our studies in the C_{60}—Co and C_{60}—Fe systems, it can be said that there exists very high spin polarization as a nature of the interface between FM and C_{60} or C_{60} with bonded FM atoms. This agrees with the theoretical predictions for the hybrid materials and interfaces of 3d transition metals and nanocarbons [7,8].

As for the robustness of the interface spin polarization, the strong exponential mP_{int} decrease is ascribed to the excitation of magnetic disorders in the C_{60}—Fe compound by taking account of the XMCD study on the Co-doped C_{60} films [6,18]. It can be speculated that the Fe and Co atoms covalently bonded with C_{60} would have localized d-electron spins with similar electronic and magnetic states considering the similar T_C values observed for both films. The present results claims that the formation of hybrid compounds and spinterfaces between FMs and MMs can lead to possible problems in temperature robustness instead of very high spin polarization at low temperature.

4. Summary

Spin-dependent transport property of a Fe-doped C_{60} film with a composition of $C_{60}Fe_7$ was investigated at low temperatures in the CIP geometry. The $C_{60}Fe_7$ film is suggested to possess a granular structure of the C_{60}—Fe compound matrix and small Fe nanoparticles dispersed therein. The CIP device exhibits TMR as large as 50% and it shows exponential MR–*V* dependence similar to the Co-doped C_{60} films. The *I*–*V* characteristics are associated with the 3rd–7th order cotunneling in the range of $T < 20$ K. The interface spin polarization at zero temperature is estimated to be remarkably high ($P_{int} \geq 56\%$) compared with that in Fe crystal, though it seems to be smaller than that in the Co-doped C_{60} films having the metal contents comparable to the present film. It is also suggested that the interface spin polarization in the Fe- and Co-doped films decreases exponentially with temperature in the same manner, being possibly associated with the metal atoms involved in the C_{60}-based compound. The present study suggests that the interface spin polarization cited as the major factor for efficient spin-injection can be tailored based on the molecule-level design of the MM–FM hybrid structures and spinterfaces.

Acknowledgements

The present study was partly supported by Grant-in-Aid for Scientific Research (19360290, 22740206, 22760033 and 24360266) from MEXT of Japan and by JSPS Postdoctral Fellowship for Foreign Researchers (PE12020). The authors would like to acknowledge Prof. Koki Takanashi (Tohoku Univ.), Prof. Yoshihito Maeda (Kyoto Univ.) and Dr. Seiji Mitani (NIMS) for their kind support and useful discussion.

References

[1] S. Sanvito, Nature Physics 6 (2010) 562.
[2] Y. Zhan, M. Fahlman, Journal of Polymer Science B 50 (2012) 1463.
[3] J.S. Jiang, J.E. Pearson, S.D. Bader, Physical Review B 77 (2008) 035303.
[4] M. Grünewald, M. Wahler, F. Schumann, M. Michelfeit, C. Gould, R. Schmidt, F. Würthner, G. Schmidt, L.W. Molenkamp, Physical Review B 84 (2011) 125208.
[5] T. Suzuki, M. Kurahashi, X. Ju, Y. Yamauchi, Journal of Physical Chemistry B 106 (2002) 11553.
[6] Y. Matsumoto, S. Sakai, S. Entani, Y. Takagi, T. Nakagawa, H. Naramoto, P. Avramov, T. Yokoyama, Chemical Physics Letters 511 (2011) 68.
[7] C.K. Yang, J. Zhao, J.P. Lu, Nano Letters 4 (2004) 561.
[8] Y. Mao, J. Yuan, J. Zhang, Journal of Physics: Condensed Matter 20 (2008) 115209.
[9] N. Atodiresei, J. Brede, P. Lazic', V. Caciuc, G. Hoffmann, R. Wiesendanger, S. Blügel, Physical Review Letters 105 (2010) 066601.
[10] S. Sakai, I. Sugai, S. Mitani, K. Takanashi, Y. Matsumoto, H. Naramoto, P.V. Avramov, S. Okayasu, Y. Maeda, Applied Physics Letters 91 (2007) 242104.
[11] S. Sakai, S. Mitani, I. Sugai, T. Takanashi, Y. Matsumoto, S. Entani, H. Naramoto, P. Avramov, Y. Maeda, Physical Review B 83 (2011) 174422.
[12] S. Sakai, S. Mitani, Y. Matsumoto, S. Entani, P. Avramov, M. Ohtomo, H. Naramoto, K. Takanashi, Journal of Magnetism and Magnetic Materials 324 (2012) 1970.
[13] S. Sakai, H. Naramoto, P.V. Avramov, T. Yaita, V. Lavrentiev, K. Narumi, Y. Baba, Y. Maeda, Thin Solid Films 515 (2007) 7758.
[14] D. Babonneau, J. Briatico, F. Petroff, Journal of Applied Physics 87 (2000) 3432.
[15] T.B. Tran, I.S. Beloborodov, J. Hu, X.M. Lin, T.F. Rosenbaum, H.M. Jaeger, Physical Review B 78 (2008) 075437.
[16] S. Mitani, S. Takahashi, K. Takanashi, K. Yakushiji, S. Maekawa, H. Fujimori, Physical Review Letters 81 (1998) 2799.
[17] R.J. Soulen Jr., J.M. Byers, M.S. Osofsky, B. Nadgorny, T. Ambrose, S.F. Cheng, P.R. Broussard, C.T. Tanaka, J. Nowak, J.S. Moodera, A. Barry, J.M.D. Coey, Science 282 (1998) 85.
[18] Y. Matsumoto, S. Sakai, Y. Takagi, T. Yokoyama, T. Shimada, S. Mitani, H. Naramoto, Y. Maeda, Chemical Physics Letters 470 (2009) 244.